Supplement of

Quantifying urban, industrial, and background changes in NO_2 during the COVID-19 lockdown period based on TROPOMI satellite observations

Vitali Fioletov et al.

Correspondence to: Vitali Fioletov (Vitali.Fioletov@outlook.com or Vitali.Fioletov@canada.ca)

SUPPLEMENT

Supplement A. The uncertainties and sensitivity analysis

There are three main groups of uncertainties in the described method of emission estimates. The first group is related to NO_2 retrievals themselves and include measurement random errors, errors due to the cloud cover and surface reflectivity, errors related to the uncertainties in the vertical profile and therefore in the airmass factor. The second group is related to the fitting process. These include the statistical errors, uncertainties due to assumptions about the lifetime and plume widths, and errors due to imperfection of the wind reanalysis data. Finally, there are uncertainties related to the atmospheric variability, i.e., due to the fact that the plume characteristics are different from one day to another.

The TROPOMI measurement uncertainties are well-established and are not considered here. The study is focussed on relative changes in 2020 vs. 2018-2019, the scaling-type errors such as errors in AMFs do not affect the results.

The fitting algorithm depends on two parameters: the lifetime and plume width. Since prescribed values were used for these parameters, the final results may depend on their selection. There are two issues here: how to determine the "optimal" values and what are the uncertainties associated with selection of the prescribed values. To find the most suitable lifetime value, the analysis was performed for several prescribed values between 1 and 10 hours and the standard deviation of the residuals was estimated for the 27 areas of the Canada and the U.S. region. The results are shown in Fig. S1. While the "optimal" lifetimes, i.e., those that deliver the smallest residuals, varies from area to area, on average, the smallest standard deviation corresponds to 3.3 hours. The lifetime parameter (τ) has little impact on the background values. The emissions estimates depend on $1/\tau$ and the impact is substantial for both urban and industrial components (Fig, 2s left column). However, the impact to the differences between 2020 and 2018-2019 is much smaller, typically within a few percent (Fig 2s, left).

The plume width parameter value also has impact on the emissions estimates, particularly on industrial ones. Similarly, to the lifetime sensitivity analysis, we performed the emissions estimates for several plume width values between 4 and 16 km (Fig. S3). The plume width parameter affects the emission results in two ways. First, for a point source, a wider plume width may lead to overestimation of the total mass and therefore emissions. The optimal plume width can be estimated from isolated point sources by minimizing the fitting residuals or by modelling the plume based on the satellite pixel resolution. Such estimates give a value of about 7-8 km. This effect is less important for area source emission estimates such as urban emissions. Second, a larger width value increases the correlation between plume functions making it more difficult to separate the sources. It also changes the grouping of industrial point sources into clusters as it depends on the correlation of the plume functions. In an extreme case of St. Louis, the correlation coefficients between the urban plume function and plume functions of two main industrial source clusters increased to 0.9 for 16 km plume width, while they were all below 0.5 for 8 km width. As a result, most of urban emissions from St. Louis were attributed by the regression model to the industrial sources. It produced unrealistic industrial emissions that were much higher than the reported ones. However, St. Louis is an extreme case and for most sites this effect is rather small.

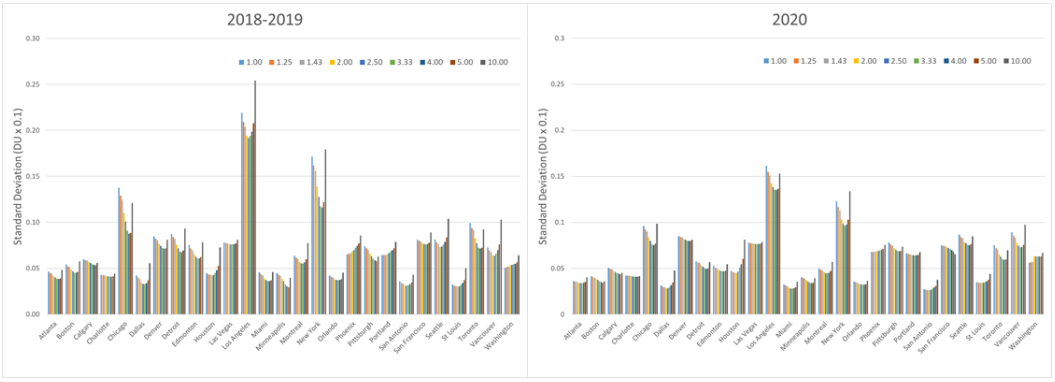

Figure S1. The standard deviation of the residuals on the residual's maps (see Figure 2c) calculated for different lifetimes for 2018-2019 and 2020. Different colors represent different lifetimes as shown in the legend. The lifetimes in hours are shown in the legend. For both time intervals, the average of standard deviations calculated for all 27 areas is the minimal for the lifetime value of 3.33 hours.

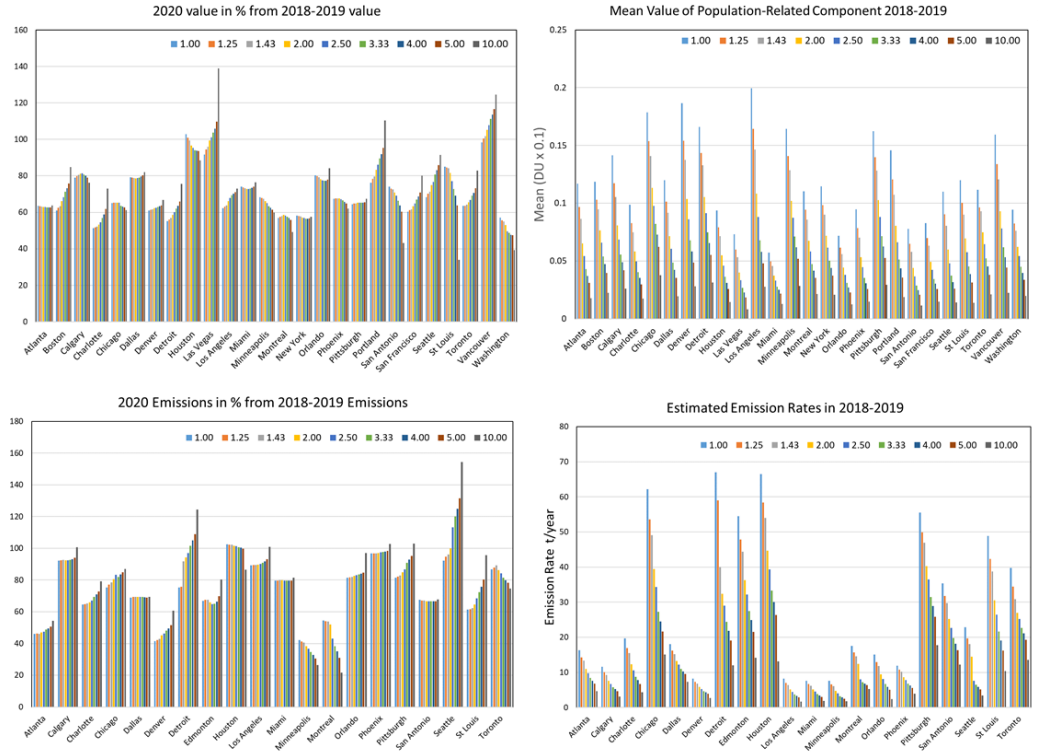

Figure S2. (left) The mean 2020 values in percent from the mean 2018-2019 values for the (top) urban, and (bottom) industrial components. (right) The mean values for 2018-2019 values for the two components. The mean values are given for annual emission per capita for the urban component and in total annual emissions for the industrial sources. The lifetimes in hours are shown in the legend.

The overall impact of the plume width on the relative changes (2020 vs. 2018-2019) is even smaller (Fig. S3, left). Based on the estimates shown in Fig. S2 and S3, it was estimated that a 1-hour deviation from the used value (3.33 hour) produce a relative change of about 1%. in urban emissions averaged over all areas in the region. Similarly, a 2 km change in the plume width leads to a 1% change in the averaged urban emissions.

Statistical errors related to the fitting procedure are relatively small due to a very large number of satellite pixels used in the fit. For the urban emissions determined by just one parameter, they are between 2% and 10% for the cities analysed in this study. However, such uncertainty estimates are based on the assumption that the residuals are not correlated that may not be the case. For this reason, we used a different approach to estimate the overall uncertainties based on estimates for 2018 and 2019. The difference between the emissions and background values estimated separately for 2018 and 2019 can be used as a measure of the uncertainty: if the standard deviation of the estimate based on data from one year is σ, then the standard deviation of the difference is $\sqrt{2}\sigma$. The uncertainty of such estimate for one area is very large, but is we assume that σ is the same for all areas within one the region, then the estimate is more reliable. The results are shown in Table S1. The standard deviations of the mean values for March 16 – June 15 due to the natural variability is 7%-17% and 5%-10% for the urban and background components respectively. For the industrial component, the values are between 10% and 30%.

Table S1. The standard deviations of interannual variability of urban and industrial emissions and the background component for the period March 16 – June 15 for different regions estimated from 2018 and 2019 data. The values are in percent of the 2018-2019 average.

Region	Urban emissions	Industrial emissions	Background
Africa	12.8	10.5	6.0
Australia and New Zealand	14.6	12.2	4.6
Canada and U.S.	9.8	13.6	6.0
Central America	6.9	10.5	4.9
China	17.1	15.8	6.5
Europe (EU) - 1	13.3	26.3	4.8
Europe (EU) - 2	11.1	16.0	4.7
India	14.0	11.5	8.3
Japan, Korea, Taiwan	15.3	10.3	5.5
Middle East	18.6	13.0	7.4
Northern Eurasia	14.6	16.2	9.7
South America	10.6	15.2	6.8
South-East Asia	15.9	30.4	6.5

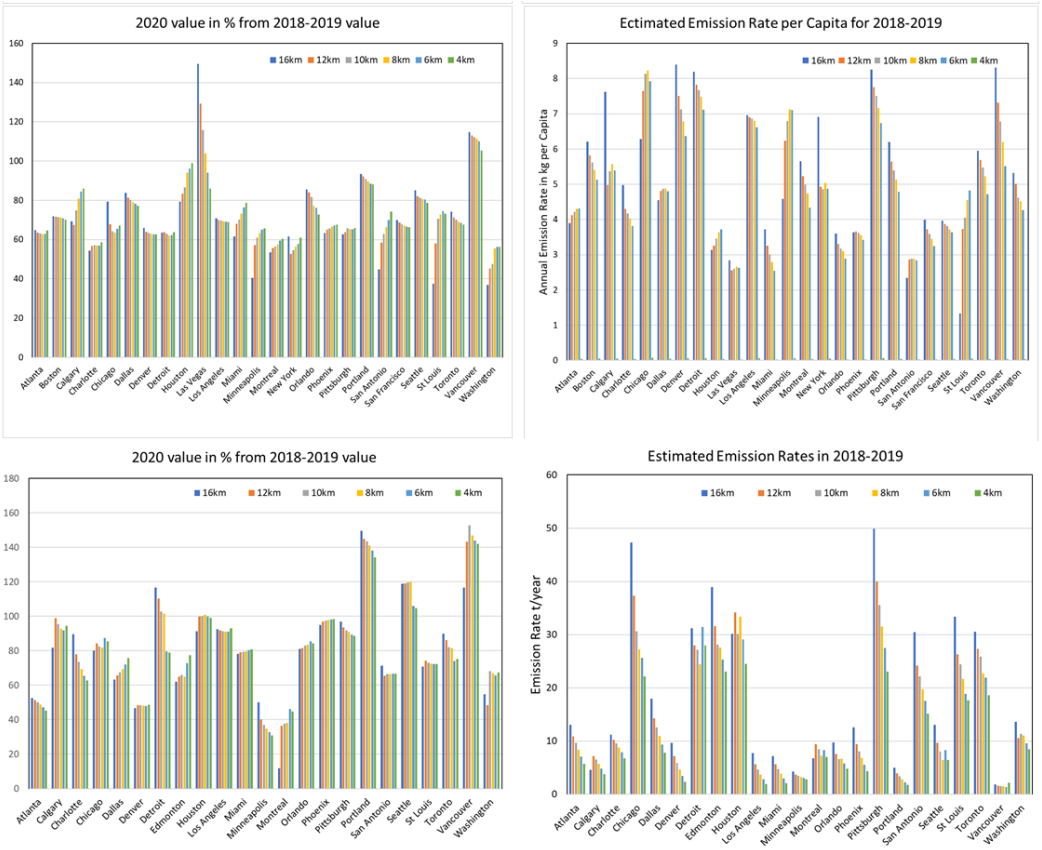

Figure S3. (left) The mean 2020 values in percent from the mean 2018-2019 values for the (top) background-, (middle) population-, and (bottom) industrial source-related components. (right) The mean values for 2018-2019 values for the three components. The mean values are given for mean NO_2 VCD for the background component, annual emission per capita for the population density-related component and in total annual emissions for the industrial sources. Different colors represent different plume widths as shown in the legend.

Supplement B. Estimates with different lifetimes for the Edmonton area

The Edmonton case shows some limitations of the method: The urban and industrial contributions cannot be reliable separated and the lifetimes of urban and some industrial sources may be different. While the regression model can successfully reproduce NO_2 distribution and the residuals are low, the interpretation of the result is complicated. There is a cluster of two industrial sources in the Edmonton city itself and the correlation between the plume functions for this cluster and the plume function of the population density-related component is 0.94. That means that the plume functions for the city and for the two industrial sources are nearly identical resulting in unreliable emission estimates. We excluded these industrial sources from the model by setting the corresponding α_i coefficients to zero, however, this leads to overestimation of population density-related emissions. Another complication is related to the cluster of three power plants east of Edmonton. Fitted total emissions are 21 kt/yr whereas 2018 reported (NPRI) emissions are 32 kt/yr, making them collectively one of the largest NO_x sources in North America. The NO_2 VCDs over the power plants when estimated from reported emissions would be larger than those observed by TROPOMI. In order to reconcile these differences, the NO_2 lifetime would need to be reduced from 3.3 to 2.5 hours. However, this shorter lifetime produces larger differences between these two characteristics for the cluster of industrial sources north-East of Edmonton (see Fig. S4). This suggest that there might be some errors associated with the assumption of a constant NO_2 lifetime, which depends on local chemical conditions and its concentration, and thus varies from source to source even within one area. Another possible explanation of the difference is related to the wind height. We used winds averaged through the lowest 1 km, which would not reflect the higher winds for at the power plant stacks relative to near-surface urban emissions. This would have the same impact on the power plant emission estimates as a shorter lifetime. While the estimated NO_2 mass is practically independent on the prescribed lifetime, it affects the emission estimates E since $E=\alpha/\tau$, where τ is lifetime and α is the total mass near the source. This possible lifetime error also should not affect the relative change estimates (2020 vs. 2018-2019) as long as the lifetime remains constant. Edmonton is probably an extreme case since three very large sources are located along the dominant wind direction, upwind of the city.

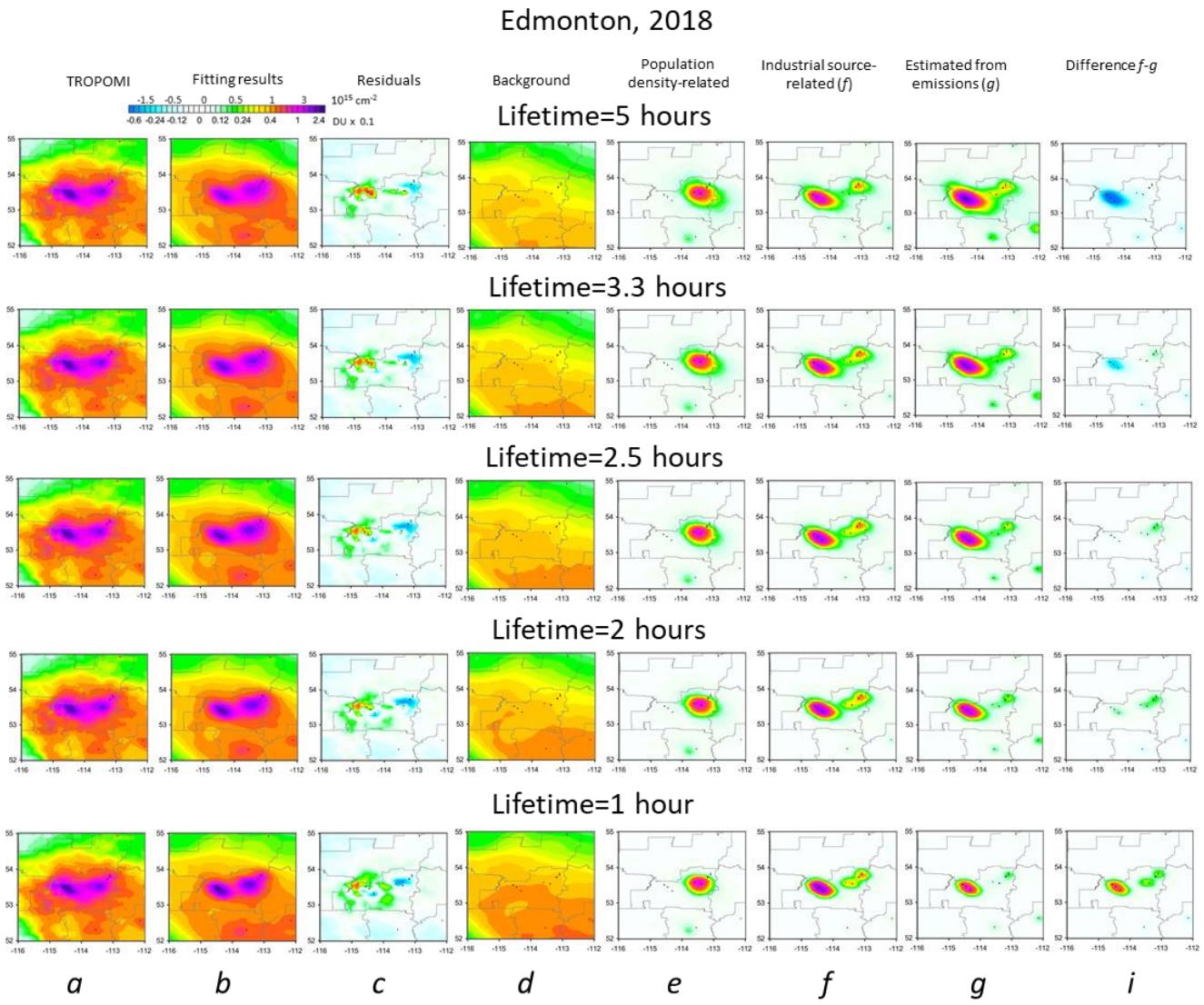

Figure S4. Similar for Figure 4, but it shows results for the Edmonton area in 2018 for five different values of assumed lifetime as indicated. The columns represent: mean TROPOMI NO_2 values, (column *a*), the fitting results (*b*), the residuals (*c*) and well as individual components of the fitting: the elevation-related (*d*), the population density-related (*e*), and the industrial sources-related (*f*). VCDs estimated from reported emissions are in column (*g*) and the difference between columns *f* and *g* is in column *i*. The *i*-column shows that expected NO_2 VCDs based on reported emissions from 3 power plants east of Edmonton are largely overestimates for the lifetime value of 5 h (the differences with TROPOMI data are negative) and largely underestimated for 1 h (the differences are clearly positive).

Supplement C. Comparison with emissions estimates from Lange et al., 2021

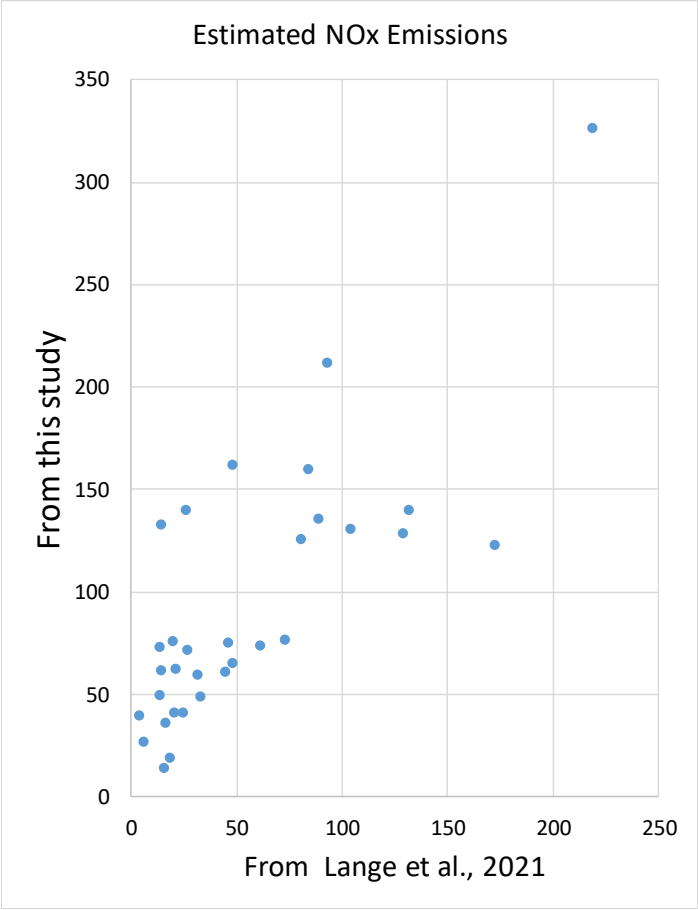

Figure S5. Estimated NO_x emissions (in mol s^{-1}) from Lange et al., 2021, and from this study. Each dot represents one large city. The correlation coefficient between the data sets is 0.78.

A recent study by Lange et al., 2021, used TROPOMI data to estimate emissions from 45 sources worldwide. This study provides emissions estimates for 33 of them. The two studies are based on the same TROPOMI data set, however, there are many differences between them: This study is based on one season (from March 16 to June 15) and not the entire year as in Lange et al., 2021. Algorithms of both studies are based on exponentially modified Gaussian (EMG) plume function, but its implementation is very different. The lifetime is estimated from the data in Lange et al., 2021, while a fixed value of 3.3 hours was used in this study. We assumed a fixed NO_2/NO_x ratio of 0.7, while Lange et al., 2021, used reanalysis data to estimate the ratio based on ozone concentrations. Finally, Lange et al., 2021, estimated emissions for a large point sources, while total emissions for 3° by 4° areas were estimated in this study. To compare the two data sets we calculated total emissions, i.e. the sum of urban and industrial emissions, and then converted them to the same lifetimes as in Lange et al., 2021, and then divided them by 0.7 to calculate NO_x emission. The results are shown in Fig. S5. There is a good correlation between the two estimates. As expected, the emission estimated in this study are higher than from Lange et al., 2021. This is because there is typically more than one emission source in the analysed 3° by 4° areas of this study. The only one "outlier", Tokyo, where emissions Lange et al., 2021, are higher (173 mol s^{-1}) than estimates from this study (123 mol s^{-1}). Tokyo has a very steep gradient in the background level toward the Pacific Ocean to the south-east and mountains at the north-west that, if not accounted for, may contribute to the emission estimates. The reason for relatively low urban emissions per capita in Tokyo compared to some other cities in the region may be related to a relatively small number of cars per capita in Tokyo (232) vs., for example, 497 in Hiroshima (https://knoema.com/atlas/Japan, accessed on May 3, 2021)

Supplement D. Missing emission sources.

Our algorithm is based on fitting of satellite observations with plume functions and requires a complete inventory of the sources. If some sources are missing, the algorithm would try to attribute their contribution to other proxies and the remains would appear in the residuals. This is typically a problem for small sources or sources that do not last long in time, such as some forest fires. However, ship emissions are a source that may substantially contribute to the total NO_2 mass in some areas and that is not included in this study. As an illustration, the fitting results for Singapore are shown in Fig. S6. Ship tracks are clearly seen on the original NO_2 map. They also clearly appear on the residuals map and the total NO_2 mass, associated with them is comparable to the total mass of urban NO_2. Ship tracks can be seen in Amsterdam, Lisbon, and some other areas.

Supplement E. Night lights as a proxy for urban emissions

The fitting results rely on the quality of the proxy data used in the fit. We found that in some cases, the population density data may not be very accurate. As an example, Fig. S6 shows the fitting results for Riyadh, Saudi Arabia. Riyadh is often considered as a large point source, but in fact emissions are coming from the city as well as from several large power plant around it. The available population density data levels off over a large area and do not show a clear maximum over Riyadh. Moreover, they show another "hotspot" west of the city that apparently does not correspond to any urban area and NO2 values are not elevated there. To verify the results, the calculations were repeated using night lights instead of the population density as a proxy for urban emissions. Unlike population density, the used night lights data set exhibits saturation above a certain limit and therefore may not represent NO_2 emissions well over large cities with dense population areas. To compensate for underestimation over the city core, they tend to overestimate the NO_2 signal over the suburbs. Compared to the population density proxy, the urban component, estimated from night light, is larger by about 30% while industrial and environs components are slightly smaller. However, the changes between 2018-2019 and 2020 remain the same: a noticeable decline in the urban component and practically no change in the industrial one. In general, the nightlight proxy fits the NO_2 distribution better: it does not have that hotspot west of the city seen in population density data, but correctly "explains" elevated NO_2 south-east of Riyadh.

This example prompted us to repeat the analysis for all cities with the night light proxy. The summary plot reproducing Fig. 13 is in Fig. S7. The left right columns, that shows the relative changes, are nearly identical. The estimated emissions per capita are somewhat higher for the nightlight proxy than for the population density one. The largest difference, up to 30% is in the Middle East region. It is Middle East where we seen the largest differences in NO_2 estimates between the two proxies. It is possible that the population density data over that region are not always accurate.

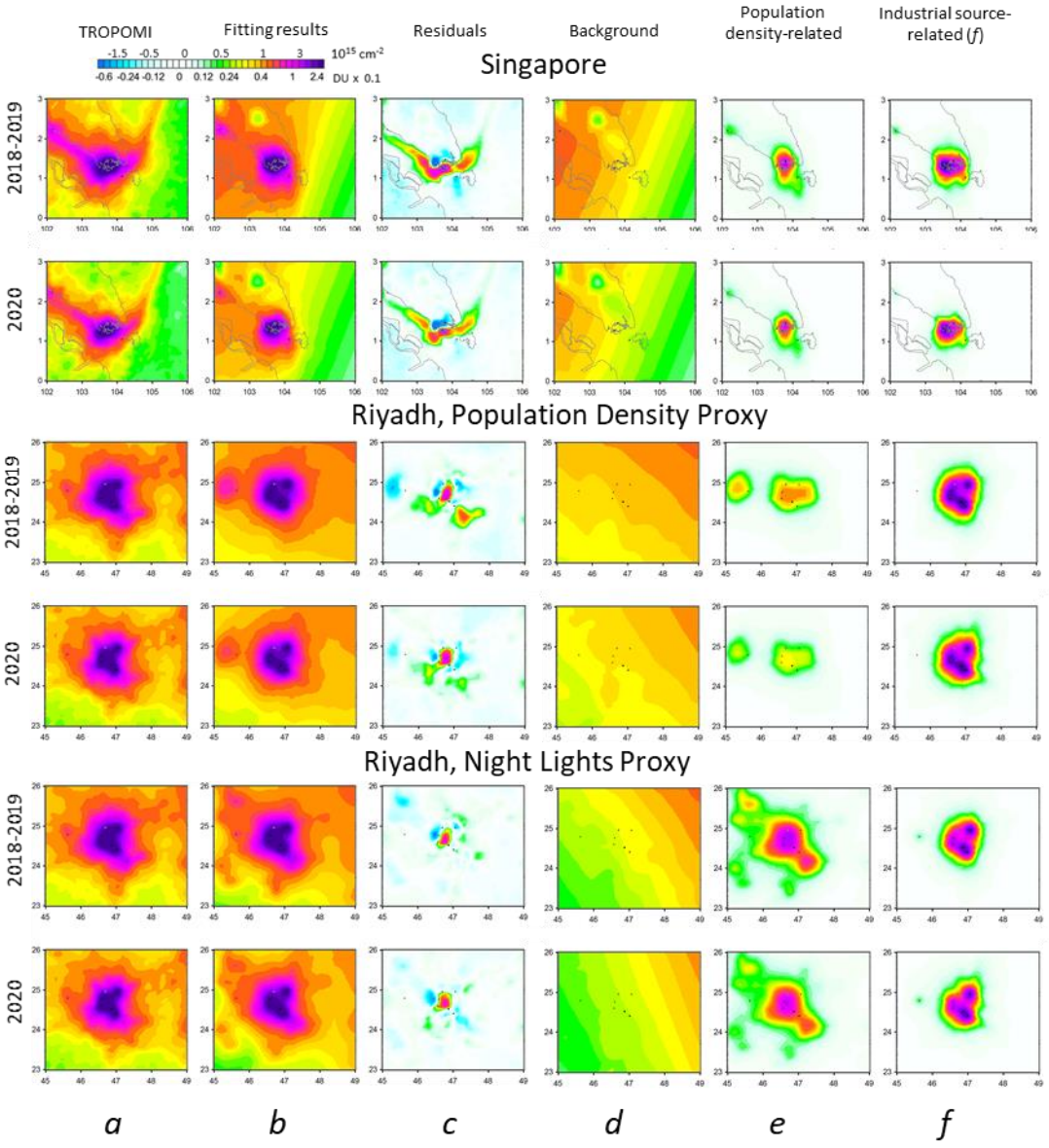

Figure S6. Similar to Figure 4 columns a-f

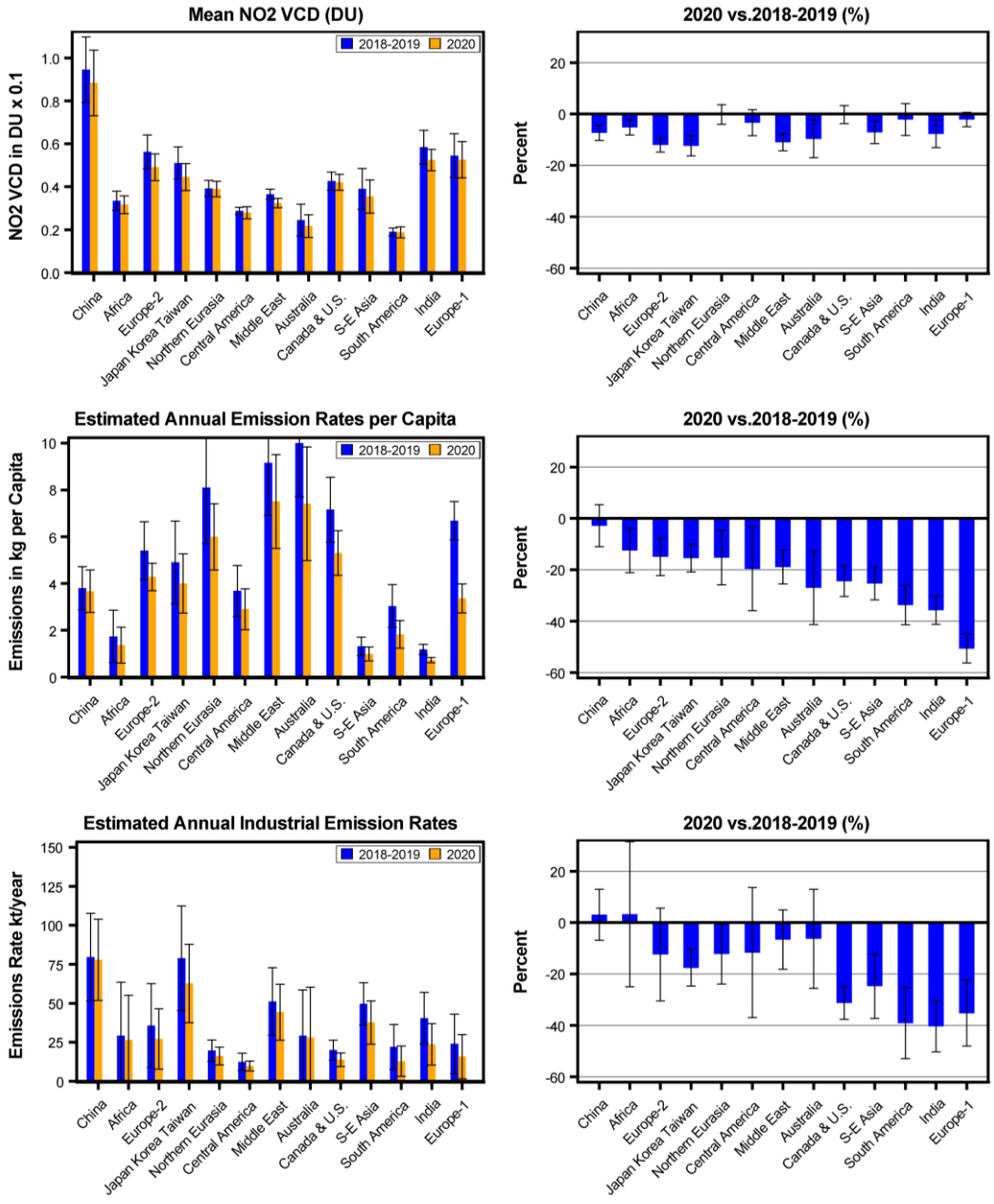

Figure S7. The same as Fig. 14, but for night lights used as a proxy for urban emissions.